THE JOURNAL OF BIOLOGICAL CHEMISTRY VOL. 289, NO. 4, pp. 1981–1992, January 24, 2014

The Role of Collagen Charge Clusters in the Modulation of Matrix Metalloproteinase Activity*

Received for publication, August 26, 2013, and in revised form, November 28, 2013 Published, JBC Papers in Press, December 2, 2013, DOI 10.1074/jbc.M113.513408

Janelle L. Lauer[‡§], Manishabrata Bhowmick[‡¶], Dorota Tokmina-Roszyk[‡¶], Yan Lin[‡], Steven R. Van Doren[‖], and Gregg B. Fields[‡¶1]

From the [‡]Department of Biochemistry, University of Texas Health Science Center, San Antonio, Texas 78229, [§]Max Planck Institute of Molecular Cell Biology and Genetics, Pfotenhauerstrasse 108, 01307 Dresden, Germany, [¶]Torrey Pines Institute for Molecular Studies, Port St. Lucie, Florida 34987 and [‖]Department of Biochemistry, University of Missouri, Columbia, Missouri 65211

Background: The role of charged clusters in modulating MMP hydrolysis of collagen is unknown.
Results: Triple-helical peptides containing charged motifs were as good or better substrates than the parent (non-charge-clustered) peptide.
Conclusion: MMP-2 and MMP-9 greatly favored the presence of charged residues.
Significance: The lack of Gly-Asp-Lys clusters in native collagens may diminish potential MMP-2 and MMP-9 collagenolytic activity.

Members of the matrix metalloproteinase (MMP) family selectively cleave collagens *in vivo*. Several substrate structural features that direct MMP collagenolysis have been identified. The present study evaluated the role of charged residue clusters in the regulation of MMP collagenolysis. A series of 10 triple-helical peptide (THP) substrates were constructed in which either Lys-Gly-Asp or Gly-Asp-Lys motifs replaced Gly-Pro-Hyp (where Hyp is 4-hydroxy-L-proline) repeats. The stabilities of THPs containing the two different motifs were analyzed, and kinetic parameters for substrate hydrolysis by six MMPs were determined. A general trend for virtually all enzymes was that, as Gly-Asp-Lys motifs were moved from the extreme N and C termini to the interior next to the cleavage site sequence, k_{cat}/K_m values increased. Additionally, all Gly-Asp-Lys THPs were as good or better substrates than the parent THP in which Gly-Asp-Lys was not present. In turn, the Lys-Gly-Asp THPs were also always better substrates than the parent THP, but the magnitude of the difference was considerably less compared with the Gly-Asp-Lys series. Of the MMPs tested, MMP-2 and MMP-9 most greatly favored the presence of charged residues with preference for the Gly-Asp-Lys series. Lys-Gly-(Asp/Glu) motifs are more commonly found near potential MMP cleavage sites than Gly-(Asp/Glu)-Lys motifs. As Lys-Gly-Asp is not as favored by MMPs as Gly-Asp-Lys, the Lys-Gly-Asp motif appears advantageous over the Gly-Asp-Lys motif by preventing unwanted MMP hydrolysis. More specifically, the lack of Gly-Asp-Lys clusters may diminish potential MMP-2 and MMP-9 collagenolytic activity. The present study indicates that MMPs have interactions spanning the P_{23}–P_{23}' subsites of collagenous substrates.

The hydrolysis of collagen (collagenolysis) is regulated on multiple levels. Features of the substrate, including its primary, supersecondary, and quaternary structure, all contribute to the efficiency at which collagen is catabolized. For example, the triple-helical supersecondary structure of collagen, which stems from its repeating Gly-Xaa-Yaa primary structure, is resistant to general proteolysis (1). Collagen quaternary structures, such as fibrils, offer more resistance to proteolytic attack than isolated triple helices (2–4).

Several members of the matrix metalloproteinase (MMP)[2] family have been recognized for their collagenolytic activity. MMPs are known to catalyze the hydrolysis of interstitial (type I–III) collagens at primarily a single site, either a Gly-Ile or Gly-Leu bond, producing ¾- and ¼-length collagen fragments (1, 5). Features of the MMP cleavage site in interstitial collagens have been investigated through a variety of approaches, including (*a*) kinetic analyses of MMP hydrolysis of native and mutant collagens and triple-helical peptide (THP) models of collagen, (*b*) biophysical studies (NMR spectroscopy and x-ray crystallography) of THPs, and (*c*) molecular dynamics simulations of triple helices (6–30). It has been noted that, although collagen has a significant distribution of charged residues, relatively few are found at the site of MMP hydrolysis (5, 31). More specifically, the overall 25-amino acid residue region surrounding the site of hydrolysis (subsites P_{13}–P_{12}') contains a maximum of two charged residues (Glu in the P_8 subsite of the α1(II) chain, Arg in the P_5' subsite of the α1(I) and α1(II) chains, and Arg in the P_8' subsite of the α1(III) chain). Sequence specificity studies show variable tolerance of charged residues by collagenolytic MMPs. Arg in the P_2' and P_8' subsites and His in the P_2' and P_4' subsites are favored, but any charged residue in the P_1' subsite is strongly disfavored (17, 32, 33).

THP studies suggest that charged residues regulate the stability of triple-helical structure (34). For example, Gly-Asp-Lys

* This work was supported, in whole or in part, by National Institutes of Health Grant CA98799 (to G. B. F.), Contract 268201000036C from the NHLBI (to G. B. F.), and Grant DE14318 from the NIDCR *Craniofacial Oral Biology Student Training in Academic Research* Program (to J. L. L.). This work was also supported by the Multiple Sclerosis National Research Institute, the Robert A. Welch Foundation, and the Texas Higher Education Science and Technology Acquisition and Retention Program (all to G. B. F.).

[1] To whom correspondence should be addressed: Torrey Pines Inst. for Molecular Studies, 11350 S. W. Village Parkway, Port St. Lucie, FL 34987. Tel.: 772-345-4724; Fax: 772-345-3647; E-mail: gfields@tpims.org.

[2] The abbreviations used are: MMP, matrix metalloproteinase; Dnp, 2,4-dinitrophenyl; FN II, fibronectin type II; fTHP, fluorogenic THP; Hyp, 4-hydroxy-L-proline; Mca, (7-methoxycoumarin-4-yl)-acetyl; MT, membrane type; THP, triple-helical peptide; RFU, relative fluorescence unit.

is destabilizing for the triple helix compared with Gly-Pro-Hyp. (Gly-Pro-Hyp)$_3$-Gly-Asp-Lys-(Gly-Pro-Hyp)$_4$-Gly-Gly had a melting temperature (T_m) value of 30.9 °C, whereas (Gly-Pro-Hyp)$_3$-Gly-Pro-Hyp-(Gly-Pro-Hyp)$_4$-Gly-Gly had a T_m value of 47.3 °C (35). In contrast, Lys-Gly-Asp offers triple-helix stability comparable with Hyp-Gly-Pro. The triple-helical peptide (Gly-Pro-Hyp)$_3$-Gly-Pro-Lys-Gly-Asp-Hyp-(Gly-Pro-Hyp)$_4$ had a T_m of 47.1 °C, which is comparable with that of (Gly-Pro-Hyp)$_3$-Gly-Pro-Hyp-Gly-Pro-Hyp-(Gly-Pro-Hyp)$_4$ (T_m = 47.3 °C) (36). Lys-Gly-Asp and Lys-Gly-Glu sequences are present in fibrillar collagens more frequently than would be expected (36). Thus, the greater frequency of Lys-Gly-(Asp/Glu) compared with Gly-(Asp/Glu)-Lys indicates an evolutionary path by which collagens retain needed stability while possessing clusters of charged residues.

As described above, within the collagen cleavage site, MMPs have little tolerance for charged residues. However, the interaction of collagen with MMPs extends over a significant length of the triple helix as modulation of MMP-1, MMP-8, MMP-13, and MT1-MMP activity was observed in THP substrates spanning subsites P_{13}–P_{17}' (17, 18, 22, 26). X-ray crystallographic and NMR spectroscopic studies of MMP-1·THP complexes also revealed extended interactions between enzyme and substrate (28, 29). Although it was noted over 3 decades ago that charged residue clusters have a unique distribution near the MMP cleavage site in type I collagen and that this distribution could influence collagenolysis (37), there are no experimental studies that have specifically addressed whether charged residue clusters impact collagen hydrolysis when present in regions surrounding the cleavage site. The present study used Gly-Asp-Lys or Lys-Gly-Asp motifs at various distances from the MMP cleavage site to examine the effects of charge clusters on MMP collagenolytic activity. A total of 11 fluorogenic THP (fTHP) substrates were assembled. The stabilities of peptides containing the two different motifs were analyzed, and kinetic parameters for substrate hydrolysis by six MMPs were determined.

MATERIALS AND METHODS

All chemicals were molecular biology or peptide synthesis grade and purchased from Fisher. The Knight single-stranded peptide (Mca-Lys-Pro-Leu-Gly-Leu-Lys(Dnp)-Ala-Arg-NH_2) was synthesized by methods described previously (38, 39). Full-length pro-MMP-2 was provided by Dr. Hideaki Nagase. MMP-9 catalytic domain was expressed as described previously (40). Pro-MMP-8 was either expressed as described (41) or purchased from Millipore (Danvers, MA) or R&D Systems (Minneapolis, MN). Pro-MMP-13 and pro-MT1-MMP (ectodomain only; no transmembrane domain) were purchased from Millipore or R&D Systems. Recombinant MMP-12 catalytic domain was produced as described (42).

Metalloproteinase Activation—All MMPs were activated by reaction with 2 mM *p*-aminomercuric acetate for 2 h at 37 °C and diluted to 20–100 nM in ice-cold Tris salt buffer + zinc (50 mM Tris, 150 mM NaCl, 0.02% NaN_3, 0.01% Brij-35, 10 mM $CaCl_2$, 1 μM $ZnCl_2$, pH 7.5) to prevent autoproteolysis. Pro-MT1-MMP was alternatively activated by incubation with 0.1 μg/ml trypsin-3 for 1 h at 37 °C. Trypsin-3 was subsequently inactivated by incubation with 1 mM 4-(2-aminoethyl)benzenesulfonyl fluoride for 15 min at room temperature. Enzyme aliquots were kept on wet ice and used the same day.

Triple-helical Substrates—All fTHPs were based on a consensus sequence derived from the collagenolytic MMP cleavage sites in human type I–III collagens (16). fTHP-15, GDK A, GDK B, GDK C, GDK D, GDK E, KGD A, KGD B, KGD C, KGD D, KGD E, α1(III)748–798 fTHP, and α1(III)748–798 KGD (see Fig. 1 and Table 1 for sequences) were synthesized by Fmoc (*N*-(9-fluorenyl)methoxycarbonyl) solid-phase chemistry as described previously (13, 17, 22, 40). Peptide synthesis was carried out on a Protein Technologies PS3 (Tucson, AZ). Peptides were cleaved from the resin using thioanisole-water-TFA (1:1:18), precipitated in methyl *tert*-butyl ether, and sedimented at 4 °C. The solvent phase was decanted.

Peptide purity was evaluated using an Agilent 1200 series analytical HPLC system (Santa Clara, CA) equipped with a 150 × 4.6-mm Vydac C_{18} column. Solvent A was 0.1% TFA, H_2O; solvent B was 0.1% TFA, acetonitrile; the gradient was 0–70% over 14 min; and the flow rate was 1 ml/min. Analytical results were used to determine the optimal preparatory gradient where 4 ml of water-dissolved peptide was injected into a Vydac C_{18} column (218TP152022) on a Varian ProStar HPLC system (Agilent). Peak fractions were analyzed via analytical HPLC and reflectance MALDI-TOF mass spectra (Voyager DE-PRO Biospectrometry Workstation, Applied Biosystems, Carlsbad, CA). Pure fractions were pooled, frozen, lyophilized, and stored at −20 °C in amber vials. MALDI-TOF MS analysis indicated a mass of 4593.1 Da for fTHP-15 (theoretical, 4589.0 Da), 4653.0 Da for GDK A (theoretical, 4655.2 Da), 4653.0 Da for GDK B (theoretical, 4655.2 Da), 4655.0 Da for GDK C (theoretical, 4655.2 Da), 4656.0 Da for GDK D (theoretical, 4655.2 Da), 4656.0 Da for GDK E (theoretical, 4655.2 Da), 4767.0 Da for KGD A (theoretical, 4767.3 Da), 4658.6 Da for KGD B (theoretical, 4655.1 Da), 4658.0 Da for KGD C (theoretical, 4655.1 Da), 4655.5 Da for KGD D (theoretical, 4655.1 Da), 4616.0 Da for KGD E (theoretical, 4612.0 Da), 5122.8 Da for α1(III)748–798 fTHP (theoretical, 5123.5 Da), and 5165.7 Da for α1(III)748–798 KGD fTHP (theoretical, 5157.6 Da).

Circular Dichroism Spectroscopy—Peptides were dissolved in Tris salt buffer and equilibrated at 4 °C (>8 h) to facilitate triple-helix formation. Peptide concentrations were determined using a Thermo Scientific NanoDrop 1000 (Waltham, MA) via a wavelength scan at λ = 363 nm, ϵ_{Dnp} = 15,900 M^{-1} cm^{-1}. Triple-helical structure was evaluated by near-UV circular dichroism (CD) spectroscopy using a Jasco J-810 spectropolarimeter (Easton, MD) with a path length of 1 mm. Thermal transition curves were obtained by recording the molar ellipticity ([θ]) at λ = 225 nm with temperature increasing by 20 °C/h from 5 to 80 °C. Temperature was controlled by a Jasco PTC-348WI temperature control unit. The peptide T_m was defined as the inflection point in the transition region (first derivative). The spectra were normalized by designating the highest $[\theta]_{225\ nm}$ as 100% folded and the lowest $[\theta]_{225\ nm}$ as 0% folded.

MMP Assays—Enzyme kinetics was determined in a Synergy H4 Hybrid Multi-Mode Microplate Reader (BioTek, Winooski, VT) at $\lambda_{excitation}$ = 324 nm and $\lambda_{emission}$ = 393 nm as described previously (40, 42). In brief, a 100 μM stock peptide solution was diluted 1:1 12 times. Peptide solution (76 μl) was loaded onto a

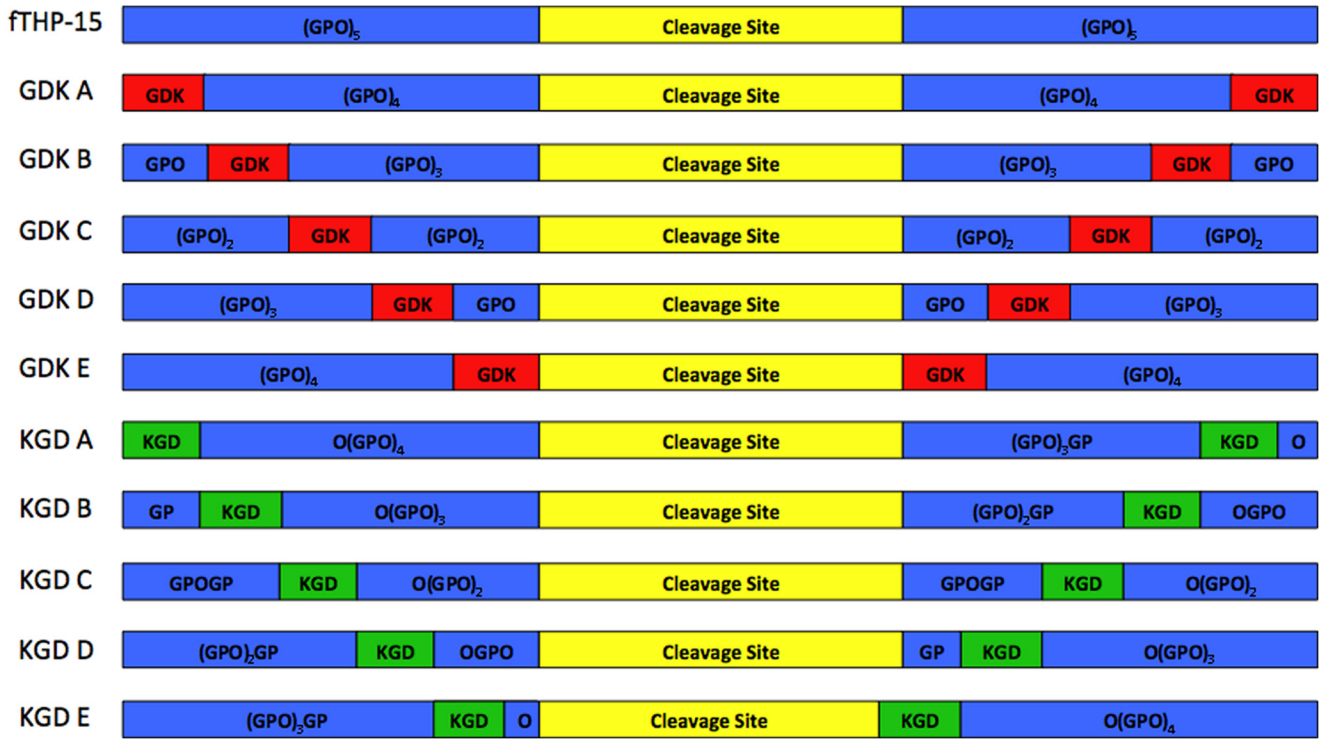

FIGURE 1. **Modular structure of fTHPs used in the present study.** The parent, fTHP, contains an MMP cleavage site (denoted in *yellow*; sequence given in Table 1) in between $(Gly\text{-}Pro\text{-}Hyp)_5$ repeats (denoted in *blue*). For the GDK series of peptides, single Gly-Pro-Hyp repeats were replaced by Gly-Asp-Lys (denoted in *red*). For the KGD series of peptides, single Hyp-Gly-Pro repeats were replaced by Lys-Gly-Asp (denoted in *green*). To properly accommodate Lys-Gly-Asp, KGD E required modification of the cleavage site sequence (see Table 1).

Nunc 384 white polystyrene well plate (Sigma-Aldrich), the plate was read, and 4 μl of 10× enzyme stock solution was added. The plate was shaken at 25 °C every 30 s, and each well was read every 8 s (for 600 s) to determine initial reaction rates. Plates were stored at ambient temperature (>24 h) before a final reading. Peptide (25 μM) was analyzed by analytical HPLC to determine the percentage of reaction completeness with 100% cleavage RFU = [(24-h RFU) − (0-h RFU)] × 100/(% peptide cleaved) where RFU is relative fluorescence unit. Enzyme activity was determined as follows: V_{Corr} = [peptide] × (initial rate)/(100% cleavage RFU). Analysis of substrate concentration *versus* reaction velocity was achieved by Lineweaver-Burke, Hanes-Woolf, and Eadie-Hofstee plots as well as non-linear regression by GraphPad Prism. When the four modes of analysis correlated well, the experiment was considered a success.

RESULTS

Eleven fTHPs were utilized in the present study (Fig. 1 and Table 1). The first (fTHP-15) incorporated a 15-residue consensus sequence from type I–III collagens (subsites P_7–P_8') and provided for convenient monitoring of triple-helical peptidase activity by collagenolytic MMP family members (16–18, 22). To examine the impact of charged residue clusters on MMP activity, one of two tripeptides, Gly-Asp-Lys or Lys-Gly-Asp, replaced a Gly-Pro-Hyp or Hyp-Gly-Pro tripeptide, respectively, within the Gly-Pro-Hyp repeat regions of fTHP-15 (Fig. 1). For example, in peptide GDK A, the Gly-Pro-Hyp tripeptides at the far N and C termini in fTHP-15 were replaced by Gly-Asp-Lys (Fig. 1). In peptide GDK B, the Gly-Asp-Lys tripeptides were located 3 residues closer to the cleavage site compared with GDK A (Fig. 1). Ultimately, peptide GDK E possessed Gly-Asp-Lys tripeptides bordering the 15-residue cleavage site (Fig. 1). In a similar fashion, peptide KGD A had the Lys-Gly-Asp tripeptides at the far N and C termini, whereas KGD E had the Lys-Gly-Asp tripeptides bordering the cleavage site (Fig. 1). To accommodate Lys-Gly-Asp while keeping the Yaa-Gly-Xaa repeating motif in the KGD E triple helix, the cleavage site was extended by 1 residue in the N-terminal direction (Hyp in subsite P_8) and reduced by 1 residue in the C-terminal direction (Arg was replaced by Lys in subsite P_8').

All 11 fTHPs exhibited CD spectra characteristic of triple-helical structures with positive $[\theta]$ values at λ = 225 nm and strongly negative $[\theta]$ values at λ = 195 nm (Fig. 2). The magnitudes of the $[\theta]_{225\ nm}$ values were similar for all peptides, indicating that the fTHPs had similar fractions of triple-helical content. Monitoring of $[\theta]_{225\ nm}$ as a function of temperature resulted in sigmoidal melting curves for all fTHPs (Figs. 3 and 4) indicative of transitions from triple helices to monomeric species (43). The T_m values for GDK A, GDK B, GDK C, GDK D, and GDK E were 47, 37, 40, 37, and 27 °C, respectively (Table 1). Thus, all of the Gly-Asp-Lys-containing peptides were less thermally stabile than the parent peptide, fTHP-15 (T_m = 55 °C), as expected based on prior studies (44). The stability was affected by the position of the Gly-Asp-Lys triplets. When a Gly-Asp-Lys triplet was substituted for a Gly-Pro-Hyp triplet at the extreme N and C termini (residues 1–3 and 43–45; GDK A), an 8 °C loss in stability was observed. Moving the Gly-Asp-Lys triplet closer to the cleavage site on each side (GDK B, GDK C,

TABLE 1

Sequences and thermal stabilities of peptides used in this study

SSP, single-stranded peptide; NA, not applicable.

Peptide	Sequence	T_m
		℃
Knight SSP	Lys(Mca)-Pro-Leu-Gly ↓ Leu-Lys(Dnp)-Ala-Arg-NH_2	NA
fTHP-15	$(Gly\text{-}Pro\text{-}Hyp)_5$-Gly-Pro-Lys(Mca)-Gly-Pro-Gln-Gly ↓ Leu-Arg-Gly-Gln-Lys(Dnp)-Gly-Val-Arg-$(Gly\text{-}Pro\text{-}Hyp)_5$-$NH_2$	55
GDK A	Gly-Asp-Lys-$(Gly\text{-}Pro\text{-}Hyp)_4$-Gly-Pro-Lys(Mca)-Gly-Pro-Gln-Gly ↓ Leu-Arg-Gly-Gln-Lys(Dnp)-Gly-Val-Arg-$(Gly\text{-}Pro\text{-}Hyp)_4$-Gly-Asp-Lys-$NH_2$	47
GDK B	Gly-Pro-Hyp-Gly-Asp-Lys-$(Gly\text{-}Pro\text{-}Hyp)_3$-Gly-Pro-Lys(Mca)-Gly-Pro-Gln-Gly ↓ Leu-Arg-Gly-Gln-Lys(Dnp)-Gly-Val-Arg-$(Gly\text{-}Pro\text{-}Hyp)_3$-Gly-Asp-Lys-Gly-Pro-Hyp-NH_2	37
GDK C	$(Gly\text{-}Pro\text{-}Hyp)_2$-Gly-Asp-Lys-$(Gly\text{-}Pro\text{-}Hyp)_2$-Gly-Pro-Lys(Mca)-Gly-Pro-Gln-Gly ↓ Leu-Arg-Gly-Gln-Lys(Dnp)-Gly-Val-Arg-$(Gly\text{-}Pro\text{-}Hyp)_2$-Gly-Asp-Lys-$(Gly\text{-}Pro\text{-}Hyp)_2$-$NH_2$	40
GDK D	$(Gly\text{-}Pro\text{-}Hyp)_3$-Gly-Asp-Lys-Gly-Pro-Hyp-Gly-Pro-Lys(Mca)-Gly-Pro-Gln-Gly ↓ Leu-Arg-Gly-Gln-Lys(Dnp)-Gly-Val-Arg-Gly-Pro-Hyp-Gly-Asp-Lys-$(Gly\text{-}Pro\text{-}Hyp)_3$-$NH_2$	37
GDK E	$(Gly\text{-}Pro\text{-}Hyp)_4$-Gly-Asp-Lys-Gly-Pro-Lys(Mca)-Gly-Pro-Gln-Gly ↓ Leu-Arg-Gly-Gln-Lys(Dnp)-Gly-Val-Arg-Gly-Asp-Lys-$(Gly\text{-}Pro\text{-}Hyp)_4$-$NH_2$	27
KGD A	Lys-Gly-Asp-Hyp-$(Gly\text{-}Pro\text{-}Hyp)_4$-Gly-Pro-Lys(Mca)-Gly-Pro-Gln-Gly ↓ Leu-Arg-Gly-Gln-Lys(Dnp)-Gly-Val-Arg-$(Gly\text{-}Pro\text{-}Hyp)_3$-Gly-Pro-Lys-Gly-Asp-Hyp-NH_2	52
KGD B	Gly-Pro-Lys-Gly-Asp-Hyp-$(Gly\text{-}Pro\text{-}Hyp)_3$-Gly-Pro-Lys(Mca)-Gly-Pro-Gln-Gly ↓ Leu-Arg-Gly-Gln-Lys(Dnp)-Gly-Val-Arg-$(Gly\text{-}Pro\text{-}Hyp)_2$-Gly-Pro-Lys-Gly-Asp-Hyp-Gly-Pro-Hyp-NH_2	51
KGD C	Gly-Pro-Hyp-Gly-Pro-Lys-Gly-Asp-Hyp-$(Gly\text{-}Pro\text{-}Hyp)_2$-Gly-Pro-Lys(Mca)-Gly-Pro-Gln-Gly ↓ Leu-Arg-Gly-Gln-Lys(Dnp)-Gly-Val-Arg-Gly-Pro-Hyp-Gly-Pro-Lys-Gly-Asp-Hyp-$(Gly\text{-}Pro\text{-}Hyp)_2$-$NH_2$	51
KGD D	$(Gly\text{-}Pro\text{-}Hyp)_2$-Gly-Pro-Lys-Gly-Asp-Hyp-Gly-Pro-Hyp-Gly-Pro-Lys(Mca)-Gly-Pro-Gln-Gly ↓ Leu-Arg-Gly-Gln-Lys(Dnp)-Gly-Val-Arg-Gly-Pro-Lys-Gly-Asp-Hyp-$(Gly\text{-}Pro\text{-}Hyp)_3$-$NH_2$	51
KGD E	$(Gly\text{-}Pro\text{-}Hyp)_3$-Gly-Pro-Lys-Gly-Asp-Hyp-Gly-Pro-Lys(Mca)-Gly-Pro-Gln-Gly ↓ Leu-Arg-Gly-Gln-Lys(Dnp)-Gly-Val-Lys-Gly-Asp-Hyp-$(Gly\text{-}Pro\text{-}Hyp)_4$-$NH_2$	43
α1(III)748–798 fTHP	$(Gly\text{-}Pro\text{-}Hyp)_7$-Gly-Pro-Lys(Mca)-Gly-Pro-Gln-Gly ↓ Leu-Arg-Gly-Gln-Lys(Dnp)-Gly-Val-Arg-$(Gly\text{-}Pro\text{-}Hyp)_5$-$NH_2$	64
α1(III)748–798 KGD fTHP	Gly-Pro-Lys-Gly-Asp-Hyp-$(Gly\text{-}Pro\text{-}Hyp)_5$-Gly-Pro-Lys(Mca)-Gly-Pro-Gln-Gly ↓ Leu-Arg-Gly-Gln-Lys(Dnp)-Gly-Val-Arg-$(Gly\text{-}Pro\text{-}Hyp)_5$-$NH_2$	60

and GDK D) resulted in a 15–18 °C loss in stability. The greatest loss in stability (28 °C) was observed when Gly-Asp-Lys was substituted for Gly-Pro-Hyp at residues 13–15 and 31–33. This result is consistent with prior predictions in which the greatest perturbation of triple-helical stability occurs when Gly-Pro-Hyp triplets do not surround the substituted site (44).

The T_m values for KGD A, KGD B, KGD C, KGD D, and KGD E were ~52, ~51, ~51, ~51, and ~43 °C, respectively (Table 1). In contrast to the Gly-Asp-Lys series, the majority of the Lys-Gly-Asp-containing peptides were of thermal stability comparable with the parent peptide, fTHP-15 (T_m = 55 °C), with the exception of KGD E, which was destabilized by ~12 °C. These results are consistent with prior studies indicating that Lys-Gly-Asp sequences offer stability comparable with Gly-Pro-Hyp (36, 44). The decreased stability for KGD E where Lys-Gly-Asp borders the cleavage site sequence may be due to unfavorable interactions between specific residues. For all 11 peptides, the melting temperatures indicated thermal stabilities suitable for MMP kinetic analyses.

The melts for the KGD THPs, the GDK-E THP, and fTHP-15 (Figs. 3 and 4) have a biphasic appearance. In the case of GDK-E, the high melting, small component (T_m ~ 59 °C) is likely from the Gly-Pro-Hyp repeats at the ends. In the cases of fTHP-15, KGD A, KGD B, and KGD C, there is a lower melting, less steep component of the curve (T_m ~ 25–30 °C) that might be the central region of the THP, which bears few Pro and Hyp residues (45). Melting in segments suggests that the "all or nothing" behavior (two-state model) attributed to triple-helical melts is oversimplified, which has been reported previously (46). Microunfolding in THPs has been described (47, 48). The lower melting components could allow greater accessibility to the MMP than the more tightly wound triplets (see later discussion). Although a single T_m may be an oversimplification of some of the curves presented herein, it nonetheless allows for the evaluation of relative stability and appropriate use of the substrates based on their stabilities.

Six MMPs were examined in the present study. Two of these (MMP-8 and MMP-13) are considered "classic collagenases" (5, 49–52), whereas MT1-MMP is a cell surface-bound MMP well recognized for its collagenolytic activity (53). Although also considered a classic collagenase, results with MMP-1 were not included in the present study as MMP-1 exhibited very low activity toward the GDK fTHPs and inconsistent behavior with the KGD fTHPs (data not shown). MMP-1 appears to be particularly sensitive to substrate charge residue clusters. Two of the other MMPs included here are the gelatinase members of the family (MMP-2 and MMP-9) shown previously to cleave interstitial collagens (54–56). The sixth enzyme, MMP-12, has been reported to hydrolyze type I and III collagens (57). The hydrolysis of fTHP-15 by each of these MMPs with the exception of MMP-12 has been reported previously (16–18, 22, 40) and occurs at the Gly ↓ Leu bond. MMP-12 hydrolysis of fTHP-15 was considerably slower than for other MMPs (Table 2) and much slower than for MMP-12 hydrolysis of an fTHP derived from type V collagen (58). The MMP-12 used herein lacks a C-terminal hemopexin-like domain, which enhances MMP-12 catalytic activity for the type V collagen fTHP (58). Nonetheless, the MMP-12 catalytic domain possesses collagenolytic activity (57, 58) and is the physiologically relevant form of MMP-12 (59), and fTHP-15 serves as a well established point of reference for all of the MMPs.

For each MMP and fTHP, k_{cat}/K_m values were determined (Table 2). Significant changes were observed in k_{cat}/K_m values in response to insertion of charge clusters. A general trend for virtually all enzymes was that, as Gly-Asp-Lys triplets were moved from the extreme N and C termini (GDK A) to the interior closer to the collagen model sequence (GDK D or GDK E), k_{cat}/K_m values increased (Table 2). Additionally, all GDK pep-

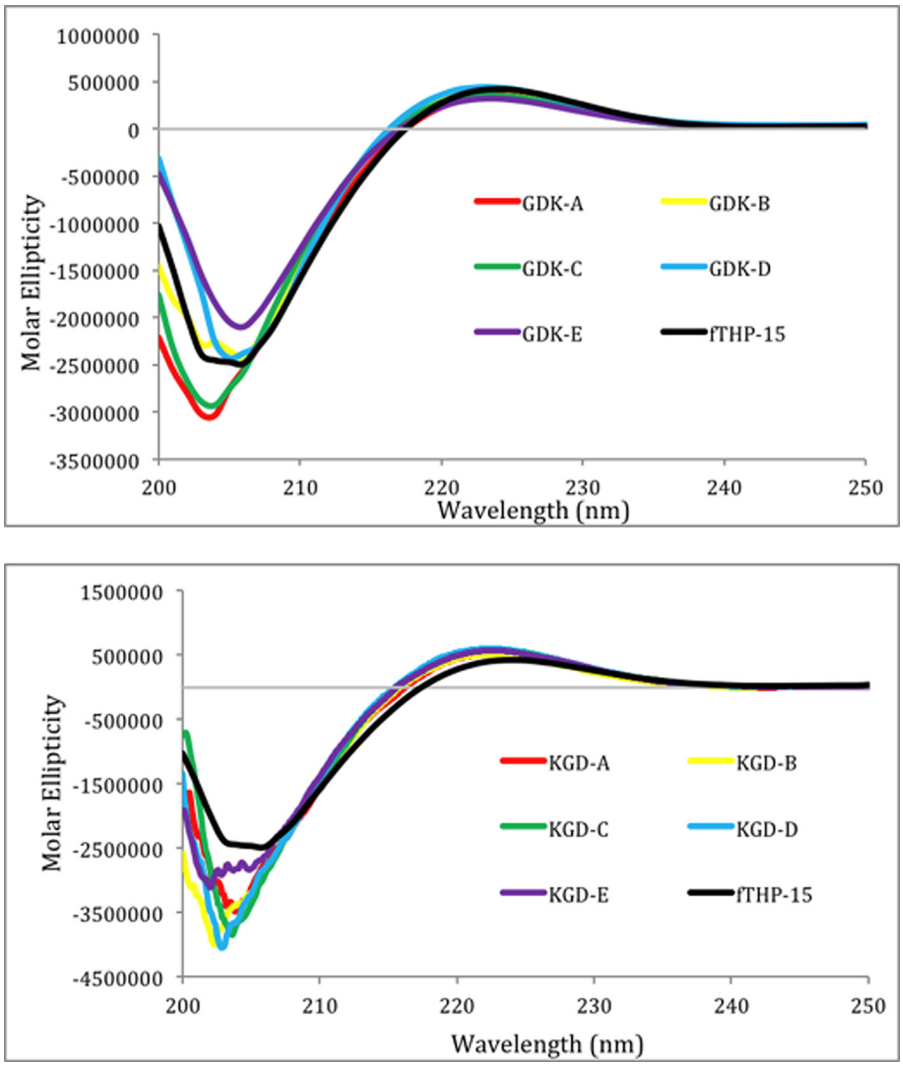

FIGURE 2. **CD spectra of fTHP-15 (*black*), GDK A (*red*), GDK B (*yellow*), GDK C (*green*), GDK D (*blue*), and GDK E (*purple*) (*top*) and fTHP-15 (*black*), KGD A (*red*), KGD B (*yellow*), KGD C (*green*), KGD D (*blue*), and KGD E (*purple*) (*bottom*).** Scans were taken from [λ] = 200–250 nm.

tides were as good or better substrates than the parent, fTHP-15. Of particular interest was the trend for the GDK B, GDK C, and GDK D peptides. The thermal stabilities of these peptides were similar (Table 1), so the increase of k_{cat}/K_m going from GDK B to GDK C to GDK D was due to the position of the charged residues, not triple-helix stability.

Data for hydrolysis of the Lys-Gly-Asp series was considerably different from data for the Gly-Asp-Lys series (Table 2). First, the highest k_{cat}/K_m values were observed when the Lys-Gly-Asp triplet was located in the middle of the Gly-Pro-Hyp repeats (KGD C) (Table 2), whereas for the Gly-Asp-Lys series, the highest k_{cat}/K_m values were observed when Gly-Asp-Lys triplets were closest to the site of hydrolysis (GDK E) (Table 2). Second, the increase in k_{cat}/K_m values for the Lys-Gly-Asp peptides compared with the parent peptide, fTHP-15 (Table 2), was considerably smaller than the increase in k_{cat}/K_m values observed for the Gly-Asp-Lys series compared with fTHP-15 (Table 2). For example, KGD C had 4.5 times the activity of fTHP-15 for MMP-2, whereas GDK E had 9.7 times the activity of fTHP-15 for the same enzyme (Table 2). In similar fashion, KGD C had 17 times the activity of fTHP-15 for MMP-9, whereas GDK E had 28 times the activity of fTHP-15 for the same enzyme (Table 2). MT1-MMP exhibited 1.1 times the activity for KGD C compared with fTHP-15 but had 5.2 times the activity for GDK E compared with fTHP-15.

Individual kinetic parameters (K_m and k_{cat}) were next examined to determine the origins of effects on overall MMP activities (Tables 3 and 4). Effects were very MMP-dependent, but some general trends emerged. For the gelatinases (MMP-2 and MMP-9), improved activity in the Gly-Asp-Lys series was due to both improved K_m and k_{cat} values (Table 3). In contrast, for MMP-8, MMP-13, and MT1-MMP, improved activity in the Gly-Asp-Lys series was due to increased k_{cat} values as K_m values were worse as Gly-Asp-Lys motifs moved closer to the cleavage site region (Table 3).

Lys-Gly-Asp motifs primarily enhanced k_{cat} with little effect on K_m for MMP-2 and MMP-9 (Table 4). Lys-Gly-Asp motifs resulted in worse K_m values and much better k_{cat} values for MMP-12, whereas for MMP-13, K_m values became worse and k_{cat} values became better as the Lys-Gly-Asp motifs were closer to the cleavage sequence (Table 4). The trade-off of K_m and k_{cat} values for MMP-8 and MT1-MMP was not particularly significant (Table 4).

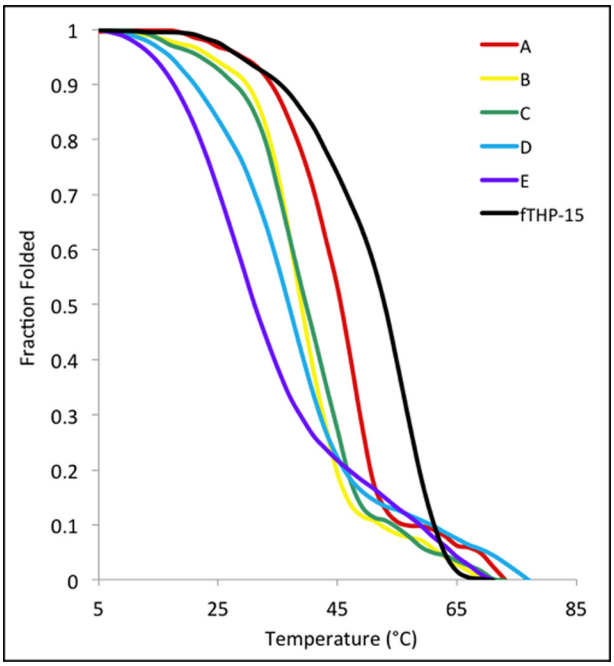

FIGURE 3. **Thermal melting curves of fTHP-15 (*black*), GDK A (*red*), GDK B (*yellow*), GDK C (*green*), GDK D (*blue*), and GDK E (*purple*).** Readings were taken at $[\theta]_{225\ nm}$ and normalized to the fraction folded.

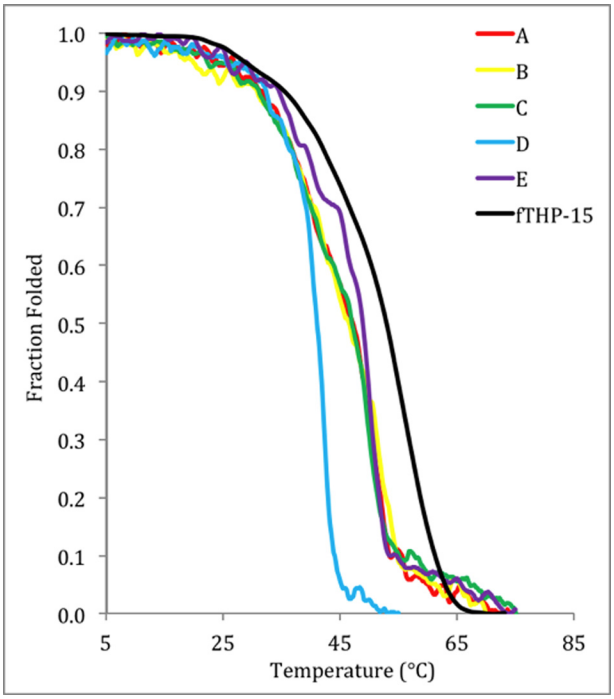

FIGURE 4. **Thermal melting curves of fTHP-15 (*black*), KGD A (*red*), KGD B (*yellow*), KGD C (*green*), KGD D (*blue*), and KGD E (*purple*).** Readings were taken at $[\theta]_{225\ nm}$ and normalized to the fraction folded.

To examine the effects of a charge cluster that occurs in native collagen, α1(III)748–798 fTHP and α1(III)748–798 KGD fTHP were synthesized (Table 1). The α1(III)748–798 KGD fTHP incorporates the Lys-Gly-Asp sequence found at residues 750–752 in native type III collagen (Table 5). The sequence of fTHP-15 was extended in the N-terminal direction with Gly-Pro-Hyp repeats to allow for the incorporation of Lys-Gly-Asp. α1(III)748–798 fTHP and α1(III)748–798 KGD fTHP formed triple helices of high thermal stability (T_m = 63.8 and 60.4 °C, respectively), which was not surprising based on their length and high composition of triple helix-stabilizing motifs (Gly-Pro-Hyp and Lys-Gly-Asp).

Hydrolysis of α1(III)748–798 fTHP and α1(III)748–798 KGD fTHP was first examined with MMP-8. k_{cat}/K_m values were 19,334 and 17,767 $s^{-1}\ M^{-1}$, respectively. Thus, the presence of the Lys-Gly-Asp triplet had little effect on MMP-8 activity. Hydrolysis of α1(III)748–798 fTHP and α1(III)748–798 KGD fTHP was then examined with MMP-9. k_{cat}/K_m values were 37,928 and 54,538 $s^{-1}\ M^{-1}$, respectively. In contrast to MMP-8, the presence of Lys-Gly-Asp increased MMP-9 activity 1.4-fold.

DISCUSSION

Collagenolytic MMPs catalyze the hydrolysis of interstitial (types I, II, and III) collagen at a single site possessing a Gly ↓ (Ile/Leu)-(Ala/Leu) motif (1). Several features of the cleavage site have been shown to contribute to MMP specificity, including the distribution of secondary amino acids (Pro and Hyp), dynamics of the peptide backbone, and overall lack of charged residues (with the primary exception of the P_5' and P_8' subsites) (1, 5, 24, 31). The interaction of MMPs with triple helices encompasses at least the P_{13}–P_{17}' subsites (26, 27, 29, 60). As interstitial collagens contain a significant number of charge clusters, the present study addressed the possible role of these charge clusters in regulating MMP activity. The substrate design featured clusters placed outside of the immediate cleavage site as (*a*) the cleavage site region in native collagens contain few charge residues and (*b*) prior studies have examined the effects of charged residues on MMP catalysis when inserted within the P_{13}–P_{12}' subsites (17, 32, 33).

The two motifs utilized here, Gly-Asp-Lys and Lys-Gly-Asp, have very different effects on the thermal stability of triple helices. The forces contributing to the lack of stabilization of triple helices by Gly-Asp-Lys and the stabilization of triple helices by Lys-Gly-Asp have been clarified. NMR spectroscopic studies have noted that axial and lateral interactions occur between charged residues with the axial interactions being the most stabilizing (34). Gly-Asp-Lys-type THPs possess two lateral salt bridges that can be formed between residues in the $i + 1, i$ positions in the leading and middle chains and middle and lagging chains (Lys → Asp) (Fig. 5) (34, 36). Although axial salt bridges are possible between residues in the $i, i + 1$ positions in the leading and middle chains and middle and lagging chains (Asp → Lys) (Fig. 5), they are not likely (36). A salt bridge is not possible between $i + 1, i$ (Lys → Asp) in the leading and lagging chains (Fig. 5) as the residues are too far apart (34, 36). The lateral Asp → Lys interactions expected in the Gly-Asp-Lys THPs evidently stabilize weakly compared with either Gly-Pro-Hyp triplets or Lys-Gly-Asp triplets.

Conversely, Lys-Gly-Asp-type THPs exhibit two axial salt bridges according to results of Hartgerink and co-workers (34). The first bridge has Lys in the *i* position in the leading chain and Asp in the $i + 2$ position in the middle chain, whereas the second bridge repeats this pattern between the middle and trailing chains (Fig. 5) (34, 61). These THPs should also exhibit lateral contact between the lagging chain and the leading chain (34).

TABLE 2
Activities of MMPs toward Gly-Asp-Lys and Lys-Gly-Asp triple-helical substrates

Peptide	MMP-2		MMP-8		MMP-9		MMP-12		MMP-13		MT1-MMP	
	k_{cat}/K_m	Relative activity[a]	k_{cat}/K_m	Relative activity[a]	k_{cat}/K_m	Relative activity[a]	k_{cat}/K_m	Relative activity[a]	k_{cat}/K_m	Relative activity[a]	k_{cat}/K_m	Relative activity[a]
	$s^{-1}{}_M{}^{-1}$	%	$s^{-1}{}_M{}^{-1}$	%	$s^{-1}{}_M{}^{-1}$	%	$s^{-1}{}_M{}^{-1}$	%	$s^{-1}{}_M{}^{-1}$	%	$s^{-1}{}_M{}^{-1}$	%
fTHP-15	120,423	100	21,753	100	69,771	100	1,953	100	31,039	100	20,784	100
GDK A	262,004	220	28,837	130	803,827	1150	5,791	300	34,067	110	19,779	100
GDK B	314,950	260	47,008	220	1,171,153	1680	7,600	390	55,973	180	33,502	160
GDK C	728,309	600	90,357	420	1,948,364	2790	15,556	800	106,861	340	71,005	340
GDK D	986,155	820	129,685	600	2,443,634	3500	18,171	930	133,115	430	108,043	520
GDK E	1,162,216	970	140,727	650	1,982,689	2840	32,557	1670	211,231	680	107,577	520
KGD A	337,988	280	18,624	86	511,077	730	4,467	230	54,890	180	24,077	116
KGD B	324,215	270	21,194	97	994,009	1430	4,846	250	59,460	190	23,486	113
KGD C	543,854	450	21,551	99	1,174,706	1680	7,827	410	98,946	320	23,012	111
KGD D	227,927	190	15,100	69	588,329	840	4,077	210	48,172	160	24,300	117
KGD E	279,035	230	22,389	103	729,451	1050	5,258	280	68,652	220	23,260	112

[a] Relative activity (%) compared with fTHP-15.

TABLE 3
Kinetic parameters for hydrolysis of Gly-Asp-Lys triple-helical substrates by MMPs

Peptide	MMP-2		MMP-8		MMP-9		MMP-12		MMP-13		MT1-MMP	
	K_m	k_{cat}	K_m	k_{cat}	K_m	k_{cat}	K_m	k_{cat}	K_m	k_{cat}	K_m	k_{cat}
	μM	s^{-1}	μM	s^{-1}	μM	s^{-1}	μM	s^{-1}	μM	s^{-1}	μM	s^{-1}
fTHP-15	5.4 ± 0.97	0.654	23.0 ± 9.4	0.500	6.4 ± 0.79	0.449	56.6 ± 0.50	0.111	21.8 ± 2.2	0.677	13.1 ± 1.6	0.300
GDK A	5.7 ± 0.79	1.485	19.4 ± 0.75	0.559	2.9 ± 0.52	2.363	26.3 ± 2.2	0.153	8.5 ± 1.12	0.289	6.9 ± 0.89	0.136
GDK B	4.5 ± 0.60	1.424	25.1 ± 2.1	1.180	2.3 ± 0.14	2.700	72.8 ± 6.3	0.554	5.9 ± 0.67	0.330	9.1 ± 0.86	0.305
GDK C	3.3 ± 0.35	2.374	18.6 ± 0.74	1.681	1.3 ± 0.22	2.621	57.4 ± 2.4	0.892	11.4 ± 0.59	1.213	8.3 ± 0.86	0.589
GDK D	2.7 ± 0.62	2.635	44.4 ± 2.4	5.758	1.7 ± 0.21	4.071	19.9 ± 3.4	0.361	25.6 ± 2.16	3.402	9.5 ± 0.29	1.026
GDK E	2.4 ± 0.42	2.804	58.5 ± 6.7	8.233	1.4 ± 0.15	2.679	32.1 ± 4.3	1.047	19.9 ± 2.0	4.197	12.0 ± 0.97	1.291

TABLE 4
Kinetic parameters for hydrolysis of Lys-Gly-Asp triple-helical substrates by MMPs

Peptide	MMP-2		MMP-8		MMP-9		MMP-12		MMP-13		MT1-MMP	
	K_m	k_{cat}	K_m	k_{cat}	K_m	k_{cat}	K_m	k_{cat}	K_m	k_{cat}	K_m	k_{cat}
	μM	s^{-1}	μM	s^{-1}	μM	s^{-1}	μM	s^{-1}	μM	s^{-1}	μM	s^{-1}
fTHP-15	5.4 ± 0.97	0.654	23.0 ± 9.4	0.500	6.4 ± 0.79	0.449	56.6 ± 0.50	0.111	21.8 ± 2.2	0.677	13.1 ± 1.6	0.300
KGD A	5.9 ± 0.94	1.987	15.8 ± 6.5	0.300	6.5 ± 0.63	3.324	91.3 ± 23.6	0.408	32.8 ± 2.3	1.803	14.1 ± 0.26	0.300
KGD B	7.1 ± 0.72	2.296	44.7 ± 26.3	0.947	4.5 ± 0.66	4.510	99.7 ± 10.8	0.483	33.8 ± 1.4	2.011	17.1 ± 3.6	0.400
KGD C	4.8 ± 0.49	2.627	30.8 ± 18.5	0.663	4.5 ± 0.96	5.335	79.0 ± 5.2	0.618	56.9 ± 3.6	5.632	15.5 ± 4.1	0.400
KGD D	9.8 ± 0.97	2.234	41.3 ± 1.5	0.623	6.6 ± 1.3	3.909	148.6 ± 13.8	0.606	120.8 ± 2.4	5.819	21.2 ± 4.5	0.500
KGD E	4.6 ± 0.60	1.290	26.7 ± 3.5	0.597	3.1 ± 0.60	2.288	83.0 ± 20.7	0.437	72.9 ± 12.4	5.005	25.1 ± 13.1	0.600

TABLE 5
Location of charge clusters in interstitial collagens

Cluster	Location[a]	No.
Gly-Asp-Lys	α2(I)418–420, α1(III)454–456, α1(III)568–570, α1(I)601–603, α1(III)604–606, α1(I)916–918, α2(I)916–918, α1(II)916–918, α1(III)919–921	9
Gly-Glu-Lys	α1(III)100–102, α1(III)328–330, α1(II)382–384, α1(II)418–420, α1(II)571–573, α1(II)601–603, α1(I)754–756, α2(I)754–756, α1(II)754–756, α2(I)922–924	10
Lys-Gly-Asp	α1(I)264–266, α1(III)456–458, α1(III)489–491, α1(I)531–533, α1(I)564–566, α1(II)564–566, α1(III)567–569, α1(I)657–659, α1(II)657–659, α1(III)750–752, α1(I)855–857, α1(II)855–857, α1(III)858–860	13
Lys-Gly-Glu	α1(III)102–104, α1(I)108–110, α2(I)108–110, α1(II)108–110, α1(III)111–113, α1(I)174–176, α2(I)174–176, α1(II)174–176, α1(III)177–179, α1(III)222–224, α2(I)264–266, α1(II)264–266, α1(III)267–269, α1(I)270–272, α2(I)270–272, α1(II)270–272, α1(III)288–290, α2(I)453–455, α2(I)531–533, α2(I)564–566, α2(I)567–569, α1(I)603–605, α1(II)603–605, α1(III)606–608, α1(I)648–650, α2(I)648–650, α1(II)648–650, α1(III)651–653, α1(III)660–662, α1(III)687–689, α1(II)756–758, α1(III)804–806, α2(I)855–857, α1(I)918–920, α2(I)918–920, α1(II)918–920, α1(III)921–923	37

[a] Numbering begins at the N terminus of the triple-helical region of each collagen.

The lateral interaction shows several possible hydrogen bonds and salt bridges (34). In view of the lower stability of Gly-Asp-Lys THPs and the structural data (34), the lateral interactions probably contribute little to triple-helix stability, and the two axial interactions (i, $i + 2$) are why Lys-Gly-Asp motifs are stabilizing for triple helices (34). In a similar fashion, Lys-Gly-Glu motifs are stabilizing, whereas Gly-Glu-Lys motifs are destabilizing (36, 62).

As expected, THP substrates where Gly-Asp-Lys motifs replaced Gly-Pro-Hyp repeats (the GDK series) were less stable than the parent THP (fTHP-15), whereas THPs with Lys-Gly-Asp motifs (the KGD series) had stability comparable with fTHP-15 (Table 1). In general, GDK A–E were better MMP substrates than KGD A–E (Table 2). Of the MMPs tested, MMP-2 and MMP-9 most greatly favored the presence of charged residues with preference for the GDK series. This preference for the GDK series could be due to the destabilization of the triple helix, sequence specificity that favors Gly-Asp-Lys over Lys-Gly-Asp, or both effects. The destabilizing Gly-Asp-Lys substitutions likely promote microunfolding of the triple helix that exposes single strands for favorable binding by MMP-2 and MMP-9, which are known to utilize their fibronec-

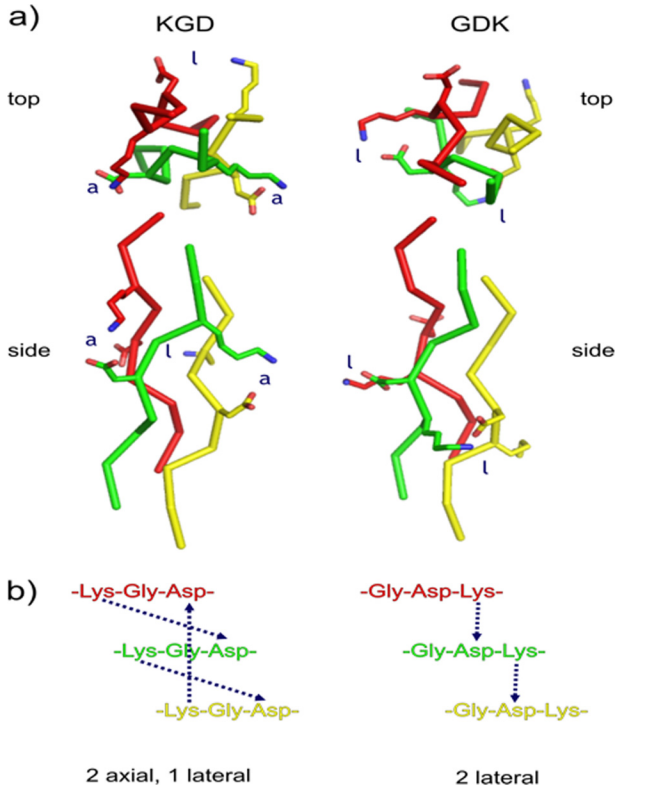

FIGURE 5. *a*, top and side views of axial and lateral interactions in Lys-Gly-Asp (*left*) and Gly-Asp-Lys (*right*) motifs. The leading strand is *red*, the middle strand is *green*, and the lagging strand is *yellow*. Three-dimensional models were built manually in PyMOL (81) using Protein Data Bank code 1CAG as a reference structure (82). The appropriate Lys and Asp rotamers causing no van der Waals overlap were selected. Models were not energy-minimized. *b*, chain alignment for Lys-Gly-Asp and Gly-Asp-Lys sequences showing axial and lateral interactions.

tin type II (FN II) inserts for gelatin binding. A prior study of collagen carbamylation indicated that destabilization of the triple helix is a contributor to relative MMP activity. Carbamylation of 11 Lys residues in type I collagen leads to a decrease in triple-helix stability (~2 °C) (63). Although the Lys residues most susceptible to carbamylation are distant from the actual MMP cleavage site (63), carbamylation results in an increase in MMP-2 activity (64). Thus, destabilization of the triple helix increases MMP-2 activity, which is analogous to what was observed in the present study.

For both MMP-2 and MMP-9, the Gly-Asp-Lys and Lys-Gly-Asp residues mostly likely interact with the FN II modules found in the catalytic domain. For example, the distance between Arg^{307}–Asp^{323} of MMP-9 FN II module 2 (residues identified as important for gelatin binding (65)) and the enzyme active site is 40–45 Å. Modeling of MMP-2 revealed a 70-Å distance between the enzyme active site and the most distal collagen interactions with FN II module 3 (66). All three MMP-2 FN II modules contribute to collagen binding with the greatest effects observed for modules 2 and 3 (and specifically Arg^{368} in module 3 and Phe^{297} in module 2) (67–69). The FN II inserts would interact with residues on the prime side of the scissile bond or zinc-binding group (70). Based on the length of a triple helix being 0.286 nm/residue, the Gly-Asp-Lys triplets would range from 26 Å (for GDK E) to 60 Å (for GDK A) from the site of hydrolysis.

The position of Lys-Gly-Asp or Gly-Asp-Lys clusters in the sequence influenced the MMP activity toward the substrate. For example, moving the Gly-Asp-Lys triplets closer to the cleavage site increased k_{cat}/K_m values. As described above, the improved activity could be due to destabilized triple helices or sequence-specific preferences for charged residues. The present study suggests some sequence specificity as GDK B, GDK C, and GDK D have similar stabilities (Table 1), but GDK D or GDK E is better for all MMPs tested (Table 2). Comparison with the KGD series indicates that improvement in activity is dependent upon both the location and nature of the cluster. For example, KGD C is the best substrate in the KGD series for the MMPs tested except for MT1-MMP (Table 2). The most favored position for Lys-Gly-Asp motifs is not as close to the cleavage site as Gly-Asp-Lys motifs. Improvements in activity, regardless of the charged motif, were manifested in k_{cat} values.

The MMP activity correlated with the destabilization by the Gly-Asp-Lys triplet, which increased with proximity to the central sequence having fewer Pro/Hyp residues. The activity of MMP-8, MMP-12, MMP-13, or MT1-MMP grew 5–6-fold in the progression from GDK-A through GDK-E (Table 2). This is consistent with the hypothesis of localized melting of sites (44, 71, 72) susceptible to proteolysis with collagenolytic MMPs, which has been suggested by molecular dynamics simulations of THPs that manifest localized separation of a chain from the triple helix with disruption of a few interchain hydrogen bonds around the scissile bond (14, 21, 73). The five triplets encompassing the scissile bond (in this study) could become more likely to melt and release a chain the closer the Gly-Asp-Lys triplet is placed. Conversely, the Lys-Gly-Asp motif, being much less destabilizing to the triple helix (Fig. 4), might account for the smaller effects of the position of the Lys-Gly-Asp triplet on catalytic efficiency, which are limited to less than 2.2-fold (Table 2). Thus, destabilization of the triple helix by Gly-Asp-Lys motifs could be a dominant contributor to triple-helical peptidase activity but a much smaller issue with the relatively stable Lys-Gly-Asp motifs.

Lys-Gly-(Asp/Glu) motifs are more common than Gly-(Asp/Glu)-Lys motifs in interstitial collagens (50 *versus* 19) (Fig. 6 and Table 5). A comparison of potential MMP cleavage site sequences in interstitial collagens, based on the Gly ↓ (Leu/Ile)-(Leu/Ala) motif (Table 6), with charge clustering (Table 5) reveals that Lys-Gly-(Asp/Glu) motifs are found closer to potential cleavage sites then Gly-(Asp/Glu)-Lys motifs (Fig. 6). For example, in homotrimeric (type II and III) collagens, Lys-Gly-(Asp/Glu) motifs are found within 30 residues or less of five potential MMP cleavage sites (Fig. 6). In contrast, Gly-(Asp/Glu)-Lys motifs are never found closer to potential cleavage sites than Lys-Gly-(Asp/Glu) motifs in these homotrimeric collagens (Fig. 6). For heterotrimeric type I collagen, the Lys-Gly-(Asp/Glu) motif is found closer to one potential cleavage site than Gly-(Asp/Glu)-Lys for the α1(I) chain, whereas the Gly-(Asp/Glu)-Lys motif is found closer to three potential cleavage sites than the Lys-Gly-(Asp/Glu) motif in the α2(I) chain (Fig. 6). Notably, in the α1(I) and α2(I) chains, Gly-(Asp/Glu)-Lys motifs are positioned 21 residues to the N-terminal side of the principal ¾-¼ cleavage site (at residues 775 and 776) (Fig. 6). As Lys-Gly-Asp is not as favored by MMPs as Gly-Asp-Lys, the

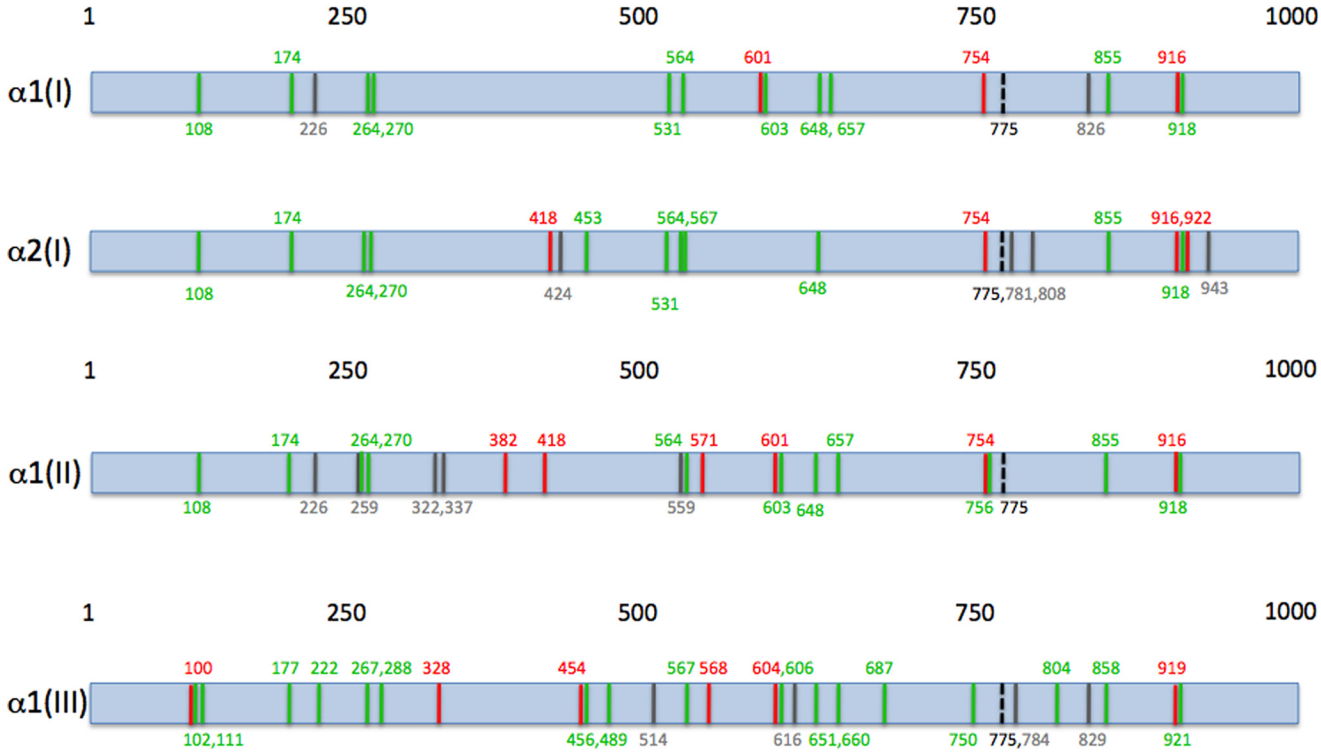

FIGURE 6. **Schematic representation of α1(I), α2(I), α1(II), and α1(III) collagen chains where potential MMP cleavage sites are indicated by *gray lines*, MMP cleavage sites are indicated by *black dashed lines*, Lys-Gly-(Asp/Glu) sites are indicated by *green lines*, and Gly-(Asp/Glu)-Lys sites are indicated by *red lines*.** Numbering begins at the N terminus of the triple-helical region of each collagen. The distance between motifs and cleavage sites are not to scale.

TABLE 6
Potential MMP cleavage sites in interstitial collagens

Cluster	Location[a]
Gly-Ile-Ala	α1(I)226–228, α1(II)226–228, α1(II)259–261, α1(II)559–561, α1(III)616–618, **α1(I)775–777**, **α1(III)775–777**, α2(I)808–810, α2(I)943–945
Gly-Leu-Ala	α1(II)322–324, α1(II)337–339, α2(I)424–426, α1(III)514–516, **α1(II)775–777**, α1(III)784–786, α1(I)826–828, α1(III)829–831
Gly-Leu-Leu	**α2(I)775–777**
Gly-Ile-Leu	α2(I)781–783

[a] Numbering begins at the N terminus of the triple-helical region of each collagen. Bold indicates actual cleavage sites.

Lys-Gly-Asp motif appears advantageous over the Gly-Asp-Lys motif not only for keeping the appropriate collagen stability but also by preventing unwanted MMP hydrolysis. More specifically, the lack of Gly-Asp-Lys clusters may diminish potential MMP-2 and MMP-9 activity. Although the α2(I) chain is the one case where Gly-(Asp/Glu)-Lys motifs are closer to potential cleavage sites than Lys-Gly-(Asp/Glu) motifs, there is only one copy of this chain in type I collagen, and the analogous potential cleavage sites are not found in the α1(I) chain.

To test whether charge clusters could influence MMP activity over the distances noted above in native collagens, two fTHPs were synthesized that modeled the 24-residue span between the Lys-Gly-Asp cluster observed at positions 750–752 in type III collagen and the MMP cleavage site at positions 775–776. MMP-8 hydrolysis was not affected by the presence of Lys-Gly-Asp in similar fashion to what was generally observed with the KGD series of peptides (Table 2). MMP-9 activity was enhanced by the presence of Lys-Gly-Asp in similar fashion to the KGD series (Table 2). Thus, the presence of Lys-Gly-Asp, even at a significant distance from the MMP cleavage site found in native collagens, modulated MMP-9 hydrolysis of triple helices.

MMP-12 behaves in a fashion similar to MMP-2 and MMP-9 in terms of regulation of activity by charge clustering (Table 2). However, MMP-12 cannot have the same extended interactions with substrate as MMP-2 and MMP-9 because MMP-12 does not possess the fibronectin type II inserts that MMP-2 and MMP-9 utilize to bind collagens (1). Prior studies showed that the MMP-12 catalytic domain possesses collagenolytic activity (57), and this domain provides contacts outside of the active site cleft (exosites) that participate in collagenolysis (58, 74). As one of the proposed contacts involves Lys^{241} of MMP-12, its interactions with charge clusters might differ from those of the collagenases (MMP-1, MMP-8, MMP-13, and MT1-MMP) and gelatinases (MMP-2 and MMP-9).

The present study indicates that MMPs have extensive long range interactions with collagenous substrates. Based on the positioning of the charged motifs, modulation of MMP activities spans the P_{23}–P_{23}' subsites. Collagenolytic MMPs have been shown to exhibit a range of conformations in solution, including those in which an "open" form of the enzyme (where the overall radius of gyration (R_g) is 28.5–29.0 Å) interacts with the triple helix (28, 60, 75). The predominant form of MMP-1 in solution is an open conformation positioned to interact with collagen (76). Thus, extensive interactions occur between an open MMP conformation and triple-helical residues.

Recombinant bacterial collagen has been utilized to examine the extent of MMP-1 interaction with the cleavage site in interstitial collagens (27). An extended cleavage site was found to participate in MMP-1 collagenolysis, consistent with prior

observations based on fTHP substrates (26). The bacterial collagen was stabilized by charge clusters (as Pro was not modified to Hyp), and as presented herein, charge clustering can also modulate MMP activity.

MMP substrates have been developed for *in vivo* analysis of MMP activity (77, 78). One of the key considerations for these probes is the selectivity of the substrate (77, 78). Our group has previously described a THP fluorescence resonance energy transfer substrate that is selective for MMP-2, MMP-9, and MMP-12 (58, 79). This substrate has subsequently been utilized for optical imaging of MMP-2/MMP-9 activity *in vivo* (80). Modification of the imaging agent by substitution of Lys-Gly-Asp sequences as exemplified by KGD C could further enhance its activity and selectivity while not sacrificing thermal stability of the triple helix. In general, the Lys-Gly-Asp motif could be used to improve solubility of triple-helical peptide probes while still offering the stability of Hyp-Gly-Pro sequences.

Acknowledgment—We thank Dr. Maciej Stawikowski for the construction of Fig. 5.

REFERENCES

1. Fields, G. B. (2013) Interstitial collagen catabolism. *J. Biol. Chem.* **288,** 8785–8793
2. Welgus, H. G., Jeffrey, J. J., and Eisen, A. Z. (1981) Human skin fibroblast collagenase: assessment of activation energy and deuterium isotope effect with collagenous substrates. *J. Biol. Chem.* **256,** 9516–9521
3. Birkedal-Hansen, H., Taylor, R. E., Bhown, A. S., Katz, J., Lin, H.-Y., and Wells, B. R. (1985) Cleavage of bovine skin type III collagen by proteolytic enzymes. *J. Biol. Chem.* **260,** 16411–16417
4. Sarkar, S. K., Marmer, B., Goldberg, G., and Neuman, K. C. (2012) Single-molecule tracking of collagenase on native type I collagen fibrils reveals degradation mechanism. *Curr. Biol.* **22,** 1047–1056
5. Fields, G. B. (1991) A model for interstitial collagen catabolism by mammalian collagenases. *J. Theor. Biol.* **153,** 585–602
6. Wu, H., Byrne, M. H., Stacey, A., Goldring, M. B., Birkhead, J. R., Jaenisch, R., and Krane, S. M. (1990) Generation of collagenase-resistant collagen by site-directed mutagenesis of murine pro α1(I) collagen gene. *Proc. Natl. Acad. Sci. U.S.A.* **87,** 5888–5892
7. Hasty, K. A., Wu, H., Byrne, M., Goldring, M. B., Seyer, J. M., Jaenisch, R., Krane, S. M., and Mainardi, C. L. (1993) Susceptibility of type I collagen containing mutated α1(I) chains to cleavage by human neutrophil collagenase. *Matrix* **13,** 181–186
8. Fan, P., Li, M. H., Brodsky, B., and Baum, J. (1993) Backbone dynamics of $(Pro\text{-}Hyp\text{-}Gly)_{10}$ and a designed collagen-like triple-helical peptide by ^{15}N NMR relaxation and hydrogen-exchange measurements. *Biochemistry* **32,** 13299–13309
9. Kramer, R. Z., Bella, J., Mayville, P., Brodsky, B., and Berman, H. M. (1999) Sequence dependent conformational variations of collagen triple-helical structure. *Nat. Struct. Biol.* **6,** 454–457
10. Lauer-Fields, J. L., Nagase, H., and Fields, G. B. (2000) Use of Edman degradation sequence analysis and matrix-assisted laser desorption/ionization mass spectrometry in designing substrates for matrix metalloproteinases. *J. Chromatogr. A* **890,** 117–125
11. Lauer-Fields, J. L., Tuzinski, K. A., Shimokawa, K.-i., Nagase, H., and Fields, G. B. (2000) Hydrolysis of triple-helical collagen peptide models by matrix metalloproteinases. *J. Biol. Chem.* **275,** 13282–13290
12. Ottl, J., Gabriel, D., Murphy, G., Knäuper, V., Tominaga, Y., Nagase, H., Kröger, M., Tschesche, H., Bode, W., and Moroder, L. (2000) Recognition and catabolism of synthetic heterotrimeric collagen peptides by matrix metalloproteinases. *Chem. Biol.* **7,** 119–132
13. Lauer-Fields, J. L., Broder, T., Sritharan, T., Chung, L., Nagase, H., and Fields, G. B. (2001) Kinetic analysis of matrix metalloproteinase triple-helicase activity using fluorogenic substrates. *Biochemistry* **40,** 5795–5803
14. Stultz, C. M. (2002) Localized unfolding of collagen explains collagenase cleavage near imino-poor sites. *J. Mol. Biol.* **319,** 997–1003
15. Fiori, S., Saccà, B., and Moroder, L. (2002) Structural properties of a collagenous heterotrimer that mimics the collagenase cleavage site of collagen type I. *J. Mol. Biol.* **319,** 1235–1242
16. Minond, D., Lauer-Fields, J. L., Nagase, H., and Fields, G. B. (2004) Matrix metalloproteinase triple-helical peptidase activities are differentially regulated by substrate stability. *Biochemistry* **43,** 11474–11481
17. Minond, D., Lauer-Fields, J. L., Cudic, M., Overall, C. M., Pei, D., Brew, K., Visse, R., Nagase, H., and Fields, G. B. (2006) The roles of substrate thermal stability and P2 and P1′ subsite identity on matrix metalloproteinase triple-helical peptidase activity and collagen specificity. *J. Biol. Chem.* **281,** 38302–38313
18. Minond, D., Lauer-Fields, J. L., Cudic, M., Overall, C. M., Pei, D., Brew, K., Moss, M. L., and Fields, G. B. (2007) Differentiation of secreted and membrane-type matrix metalloproteinase activities based on substitutions and interruptions of triple-helical sequences. *Biochemistry* **46,** 3724–3733
19. Ravikumar, K. M., Humphrey, J. D., and Hwang, W. (2007) Spontaneous unwinding of a labile domain in a collagen triple-helix. *J. Mech. Mater. Struct.* **2,** 999–1010
20. Ravikumar, K. M., and Hwang, W. (2008) Region-specific role of water in collagen unwinding and assembly. *Proteins* **72,** 1320–1332
21. Nerenberg, P. S., and Stultz, C. M. (2008) Differential unfolding of α1 and α2 chains in type I collagen and collagenolysis. *J. Mol. Biol.* **382,** 246–256
22. Lauer-Fields, J. L., Chalmers, M. J., Busby, S. A., Minond, D., Griffin, P. R., and Fields, G. B. (2009) Identification of specific hemopexin-like domain residues that facilitate matrix metalloproteinase collagenolytic activity. *J. Biol. Chem.* **284,** 24017–24024
23. Williams, K. E., and Olsen, D. R. (2009) Matrix metalloproteinase-1 cleavage site recognition and binding in full-length human type III collagen. *Matrix Biol.* **28,** 373–379
24. Xiao, J., Addabbo, R. M., Lauer, J. L., Fields, G. B., and Baum, J. (2010) Local conformation and dynamics of isoleucine in the collagenase cleavage site provide a recognition signal for matrix metalloproteinases. *J. Biol. Chem.* **285,** 34181–34190
25. Salsas-Escat, R., and Stultz, C. M. (2010) Conformational selection and collagenolysis in type III collagen. *Proteins* **78,** 325–335
26. Robichaud, T. K., Steffensen, B., and Fields, G. B. (2011) Exosite interactions impact matrix metalloproteinase collagen specificities. *J. Biol. Chem.* **286,** 37535–37542
27. Yu, Z., Visse, R., Inouye, M., Nagase, H., and Brodsky, B. (2012) Defining requirements for collagenase cleavage in collagen type III using a bacterial collagen system. *J. Biol. Chem.* **287,** 22988–22997
28. Bertini, I., Fragai, M., Luchinat, C., Melikian, M., Toccafondi, M., Lauer, J. L., and Fields, G. B. (2012) Structural basis for matrix metalloproteinase 1-catalyzed collagenolysis. *J. Am. Chem. Soc.* **134,** 2100–2110
29. Manka, S. W., Carafoli, F., Visse, R., Bihan, D., Raynal, N., Farndale, R. W., Murphy, G., Enghild, J. J., Hohenester, E., and Nagase, H. (2012) Structural insights into triple-helical collagen cleavage by matrix metalloproteinase 1. *Proc. Natl. Acad. Sci. U.S.A.* **109,** 12461–12466
30. Lu, K. G., and Stultz, C. M. (2013) Insight into the degradation of type-I collagen fibrils by MMP-8. *J. Mol. Biol.* **425,** 1815–1825
31. Lauer-Fields, J. L., Juska, D., and Fields, G. B. (2002) Matrix metalloproteinases and collagen catabolism. *Biopolymers* **66,** 19–32
32. Nagase, H., and Fields, G. B. (1996) Human matrix metalloproteinase specificity studies using collagen sequence-based synthetic peptides. *Biopolymers* **40,** 399–416
33. Fields, G. B. (2010) in *Methods in Molecular Biology, Vol. 622: Matrix Metalloproteinase Protocols* (Clark, I. M., ed) 2nd Ed., pp. 393–433, Humana Press, Totowa, NJ
34. Fallas, J. A., Dong, J., Tao, Y. J., and Hartgerink, J. D. (2012) Structural insights into charge pair interactions in triple helical collagen-like proteins. *J. Biol. Chem.* **287,** 8039–8047
35. Persikov, A. V., Ramshaw, J. A., and Brodsky, B. (2000) Collagen model peptides: sequence dependence of triple-helix stability. *Biopolymers* **55,** 436–450
36. Persikov, A. V., Ramshaw, J. A., Kirkpatrick, A., and Brodsky, B. (2005)

Electrostatic interactions involving lysine make major contributions to collagen triple-helix stability. *Biochemistry* **44,** 1414–1422
37. Gross, J., Highberger, J. H., Johnson-Wint, B., and Biswas, C. (1980) in *Collagenase in Normal and Pathological Connective Tissues* (Woolley, D. E., and Evanson, J. M., eds) pp. 11–35, John Wiley & Sons, New York
38. Nagase, H., Fields, C. G., and Fields, G. B. (1994) Design and characterization of a fluorogenic substrate selectively hydrolyzed by stromelysin 1 (matrix metalloproteinase-3). *J. Biol. Chem.* **269,** 20952–20957
39. Neumann, U., Kubota, H., Frei, K., Ganu, V., and Leppert, D. (2004) Characterization of Mca-Lys-Pro-Leu-Gly-Leu-Dpa-Ala-Arg-NH_2, a fluorogenic substrate with increased specificity constants for collagenases and tumor necrosis factor converting enzyme. *Anal. Biochem.* **328,** 166–173
40. Lauer-Fields, J. L., Whitehead, J. K., Li, S., Hammer, R. P., Brew, K., and Fields, G. B. (2008) Selective modulation of matrix metalloproteinase 9 (MMP-9) functions via exosite inhibition. *J. Biol. Chem.* **283,** 20087–20095
41. Pelman, G. R., Morrison, C. J., and Overall, C. M. (2005) Pivotal molecular determinants of peptidic and collagen triple helicase activities reside in the S_3' subsite of matrix metalloproteinase 8 (MMP-8). *J. Biol. Chem.* **280,** 2370–2377
42. Palmier, M. O., and Van Doren, S. R. (2007) Rapid determination of enzyme kinetics from fluorescence: overcoming the inner filter effect. *Anal. Biochem.* **371,** 43–51
43. Fields, G. B., and Prockop, D. J. (1996) Perspectives on the synthesis and application of triple-helical, collagen-model peptides. *Biopolymers* **40,** 345–357
44. Persikov, A. V., Ramshaw, J. A., and Brodsky, B. (2005) Prediction of collagen stability from amino acid sequence. *J. Biol. Chem.* **280,** 19343–19349
45. Ackerman, M. S., Bhate, M., Shenoy, N., Beck, K., Ramshaw, J. A., and Brodsky, B. (1999) Sequence dependence of the folding of collagen-like peptides. *J. Biol. Chem.* **274,** 7668–7673
46. Persikov, A. V., Xu, Y., and Brodsky, B. (2004) Equilibrium thermal transitions of collagen model peptides. *Protein Sci.* **13,** 893–902
47. Liu, X., Siegel, D. L., Fan, P., Brodsky, B., and Baum, J. (1996) Direct NMR measurement of the folding kinetics of a trimeric peptide. *Biochemistry* **35,** 4306–4313
48. Li, Y., Kim, S., Brodsky, B., and Baum, J. (2005) Identification of partially disordered peptide intermediates through residue-specific NMR diffusion measurements. *J. Am. Chem. Soc.* **127,** 10490–10491
49. Freije, J. M., Díez-Itza, I., Balbín, M., Sánchez, L. M., Blasco, R., Tolivia, J., and López-Otín, C. (1994) Molecular cloning and expression of collagenase-3, a novel human matrix metalloproteinase produced by breast carcinomas. *J. Biol. Chem.* **269,** 16766–16773
50. Knäuper, V., López-Otin, C., Smith, B., Knight, G., and Murphy, G. (1996) Biochemical characterization of human collagenase-3. *J. Biol. Chem.* **271,** 1544–1550
51. Mitchell, P. G., Magna, H. A., Reeves, L. M., Lopresti-Morrow, L. L., Yocum, S. A., Rosner, P. J., Geoghegan, K. F., and Hambor, J. E. (1996) Cloning, expression, and type II collagenolytic activity of matrix metalloproteinase-13 from human osteoarthritic cartilage. *J. Clin. Investig.* **97,** 761–768
52. Ala-aho, R., and Kähäri, V. M. (2005) Collagenases in cancer. *Biochimie* **87,** 273–286
53. Ohuchi, E., Imai, K., Fujii, Y., Sato, H., Seiki, M., and Okada, Y. (1997) Membrane type I matrix metalloproteinase digests interstitial collagens and other extracellular matrix macromolecules. *J. Biol. Chem.* **272,** 2446–2451
54. Aimes, R. T., and Quigley, J. P. (1995) Matrix metalloproteinase-2 is an interstitial collagenase. *J. Biol. Chem.* **270,** 5872–5876
55. Patterson, M. L., Atkinson, S. J., Knäuper, V., and Murphy, G. (2001) Specific collagenolysis by gelatinase A, MMP-2, is determined by the hemopexin domain and not the fibronectin-like domain. *FEBS Lett.* **503,** 158–162
56. Bigg, H. F., Rowan, A. D., Barker, M. D., and Cawston, T. E. (2007) Activity of matrix metalloproteinase-9 against native collagen types I and III. *FEBS J.* **274,** 1246–1255
57. Taddese, S., Jung, M. C., Ihling, C., Heinz, A., Neubert, R. H., and Schmelzer, C. E. (2010) MMP-12 catalytic domain recognizes and cleaves at multiple sites in human skin collagen type I and type III. *Biochim. Biophys. Acta* **1804,** 731–739
58. Bhaskaran, R., Palmier, M. O., Lauer-Fields, J. L., Fields, G. B., and Van Doren, S. R. (2008) MMP-12 catalytic domain recognizes triple-helical peptide models of collagen V with exosites and high activity. *J. Biol. Chem.* **283,** 21779–21788
59. Shapiro, S. D., Kobayashi, D. K., and Ley, T. J. (1993) Cloning and characterization of a unique elastolytic metalloproteinase produced by human alveolar macrophages. *J. Biol. Chem.* **268,** 23824–23829
60. Arnold, L. H., Butt, L. E., Prior, S. H., Read, C. M., Fields, G. B., and Pickford, A. R. (2011) The interface between catalytic and hemopexin domains in matrix metalloproteinase-1 conceals a collagen binding exosite. *J. Biol. Chem.* **286,** 45073–45082
61. Jalan, A. A., and Hartgerink, J. D. (2013) Simultaneous control of composition and register of an AAB-type collagen heterotrimer. *Biomacromolecules* **14,** 179–185
62. Venugopal, M. G., Ramshaw, J. A., Braswell, E., Zhu, D., and Brodsky, B. (1994) Electrostatic interactions in collagen-like triple-helical peptides. *Biochemistry* **33,** 7948–7956
63. Jaisson, S., Lorimier, S., Ricard-Blum, S., Sockalingum, G. D., Delevallée-Forte, C., Kegelaer, G., Manfait, M., Garnotel, R., and Gillery, P. (2006) Impact of carbamylation on type I collagen conformational structure and its ability to activate human polymorphonuclear neutrophils. *Chem. Biol.* **13,** 149–159
64. Jaisson, S., Larreta-Garde, V., Bellon, G., Hornebeck, W., Garnotel, R., and Gillery, P. (2007) Carbamylation differentially alters type I collagen sensitivity to various collagenases. *Matrix Biol.* **26,** 190–196
65. Collier, I. E., Krasnov, P. A., Strongin, A. Y., Birkedal-Hansen, H., and Goldberg, G. I. (1992) Alanine scanning mutagenesis and functional analysis of the fibronectin-like collagen-binding domain from human 92-kDa type IV collagenase. *J. Biol. Chem.* **267,** 6776–6781
66. Falconi, M., Altobelli, G., Iovino, M. C., Politi, V., and Desideria, A. (2003) Molecular dynamics simulation of matrix metalloproteinase 2: fluctuations and time evolution of recognition pockets. *J. Comput. Aided Mol. Des.* **17,** 837–848
67. Tam, E. M., Moore, T. R., Butler, G. S., and Overall, C. M. (2004) Characterization of the distinct collagen binding, helicase and cleavage mechanisms of matrix metalloproteinase 2 and 14 (gelatinase A and MT1-MMP): the differential roles of the MMP hemopexin C domains and the MMP-2 fibronectin type II modules in collagen triple helicase activities. *J. Biol. Chem.* **279,** 43336–43344
68. Xu, X., Mikhailova, M., Ilangovan, U., Chen, Z., Yu, A., Pal, S., Hinck, A. P., and Steffensen, B. (2009) Nuclear magnetic resonance mapping and functional confirmation of the collagen binding sites of matrix metalloproteinase-2. *Biochemistry* **48,** 5822–5831
69. Mikhailova, M., Xu, X., Robichaud, T. K., Pal, S., Fields, G. B., and Steffensen, B. (2012) Identification of collagen binding domain residues that govern catalytic activities of matrix metalloproteinase-2 (MMP-2). *Matrix Biol.* **31,** 380–388
70. Overall, C. M., and Butler, G. S. (2007) Protease yoga: extreme flexibility of a matrix metalloproteinase. *Structure* **15,** 1159–1161
71. Bächinger, H. P., and Davis, J. M. (1991) Sequence specific thermal stability of the collagen triple helix. *Int. J. Biol. Macromol.* **13,** 152–156
72. Arnold, W. V., Fertala, A., Sieron, A. L., Hattori, H., Mechling, D., Bächinger, H.-P., and Prockop, D. J. (1998) Recombinant procollagen II: deletion of D period segments identifies sequences that are required for helix stabilization and generates a temperature-sensitive *N*-proteinase cleavage site. *J. Biol. Chem.* **273,** 31822–31828
73. Nerenberg, P. S., Salsas-Escat, R., and Stultz, C. M. (2008) Do collagenases unwind triple-helical collagen before peptide bond hydrolysis? Reinterpreting experimental observations with mathematical models. *Proteins* **70,** 1154–1161
74. Palmier, M. O., Fulcher, Y. G., Bhaskaran, R., Duong, V. Q., Fields, G. B., and Van Doren, S. (2010) NMR and bioinformatics discovery of exosites that tune metalloelastase specificity for solubilized elastin and collagen triple helices. *J. Biol. Chem.* **285,** 30918–30930
75. Bertini, I., Fragai, M., Luchinat, C., Melikian, M., Mylonas, E., Sarti, N., and Svergun, D. I. (2009) Interdomain flexibility in full-length matrix metalloproteinase-1 (MMP-1). *J. Biol. Chem.* **284,** 12821–12828

76. Cerofolini, L., Fields, G. B., Fragai, M., Geraldes, C. F., Luchinat, C., Parigi, G., Ravera, E., Svergun, D. I., and Teixeira, J. M. (2013) Examination of matrix metalloproteinase-1 (MMP-1) in solution: a preference for the pre-collagenolysis state. *J. Biol. Chem.* **288,** 30659–30671
77. Fields, G. B. (2008) in *The Cancer Degradome—Proteases in Cancer Biology* (Edwards, D., Hoyer-Hansen, G., Blasi, F., and Sloane, B., eds) pp. 827–851, Springer, New York
78. Knapinska, A., and Fields, G. B. (2012) Chemical biology for understanding matrix metalloproteinase function. *Chem. Bio. Chem.* **13,** 2002–2020
79. Lauer-Fields, J. L., Sritharan, T., Stack, M. S., Nagase, H., and Fields, G. B. (2003) Selective hydrolysis of triple-helical substrates by matrix metalloproteinase-2 and -9. *J. Biol. Chem.* **278,** 18140–18145
80. Akers, W. J., Xu, B., Lee, H., Sudlow, G. P., Fields, G. B., Achilefu, S., and Edwards, W. B. (2012) Detection of MMP-2 and MMP-9 activity *in vivo* with a triple-helical peptide optical probe. *Bioconjug. Chem.* **23,** 656–663
81. DeLano, W. L. (2010) *The PyMOL Molecular Graphics System*, version 1.3r1, Schrödinger, LLC, New York
82. Bella, J., Eaton, M., Brodsky, B., and Berman, H. M. (1994) Crystal and molecular structure of a collagen-like peptide at 1.9 Å resolution. *Science* **266,** 75–81